Journal of Advanced Ceramics
2015, **4**(3): 183–189
DOI: 10.1007/s40145-015-0144-2

ISSN 2226-4108
CN 10-1154/TQ

Research Article

Strong emissions of blue–yellow–red regions of La and Ti modified $KNaNbO_3$ ferroelectric ceramics

M. D. DURRUTHY-RODRÍGUEZ[a,c,*], M. HERNÁNDEZ-GARCÍA[a], J. PORTELLES[a,b], J. FUENTES[a,b], M. A. HERNÁNDEZ-LANDAVERDE[c], M. RAMÍREZ CARDONA[d], J. M. YAÑEZ-LIMÓN[c]

[a]*Departamento de Física Aplicada, Instituto de Cibernética, Matemática y Física, CITMA, 15 # 551, Vedado, La Habana, CP 10400, Cuba*
[b]*Facultad de Física, Universidad de La Habana, San Lázaro y L, Vedado, La Habana, CP 10400, Cuba*
[c]*CINVESTAV-Unidad Querétaro, IPN, Libramiento Norponiente 2000, Fracc. Real de Juriquilla, CP 76230, Querétaro, México*
[d]*Centro de Investigaciones en Ciencias de la Tierra y Materiales, Universidad Autónoma del Estado de Hidalgo, México*

Received: November 23, 2014; Revised: January 26, 2015; Accepted: February 02, 2015

Abstract: In this work, the results of the study on the optical properties of the perovskite structure ABO_3 with La^{3+} substitution for ions K^+ and Na^+ in the A site and Ti^{4+} substitution for ion Nb^{5+} in the B site are presented. The ceramics were sintered at 1100 ℃ and 1190 ℃ and formed at 10 MPa and 80 MPa. Dense ceramics were obtained with 94% of the theoretical density. The piezoresponse force microscopy (PFM) showed needle-shaped grains with a size of 30 nm for the samples formed at 10 MPa at both sintering temperatures. Apparently, the high temperature and high pressure used in formation reduced the energy of the band gap (E_g) from 3.36 to 3.09 eV. Strong emissions to 2.19, 1.86, 2.5, and 2.31 eV were obtained by exciting the samples at 325, 373, 457, and 500 nm, respectively; these emissions corresponded to blue–yellow–red regions of the visible spectrum.

Keywords: emission spectra; condense matter; ferroelectric materials; band structure; X-ray diffraction (XRD)

1 Introduction

A great effort to design new light emission devices for monitors and communications in information technology is being carried out today. Ferroelectric materials offer encouraging possibilities because of their piezoelectric characteristics and luminescence. It is known that the rare earth ions act as an important source of luminescence; therefore they are used to carry out small substitutions in a great number of materials [1–3].

Ferroelectric lanthanum-doped lead zirconate–titanate ceramics $Pb_{1-y}La_y(Zr_xTi_{1-x})O_3$ (PLZT) have been the object of intense study due to their several possible uses associated with their high transparency in optical applications. Theoretical calculations of the width of the forbidden band gap of PLZT show a direct band gap at the point Γ, $E_g = 2.29$ eV [4]. The increment of the forbidden band gap energy and the

* Corresponding author.
E-mail: dolores@icimaf.cu

optical properties are influenced by La-4f orbital and its hybridization with O-2p orbital [4–6].

Previous works showed that the La and Ti modified $KNaNbO_3$ ceramic is a ferroelectric with a paraelectric–ferroelectric phase transition around 100 ℃ and a high permittivity value at room temperature [7,8]. The present work studies the La^{3+} and Ti^{4+} effects on the optical properties of $K_{0.5}Na_{0.5}NbO_3$.

2 Experimental procedure

The samples were prepared by traditional solid state synthesis in order to obtain the stoichiometric relationship of $(K_{0.5}Na_{0.5})_{0.95}La_{0.05}Nb_{0.9}Ti_{0.05}O_{2.9}$ (abbreviated as KNNLaTi), using the reactive agent powders K_2CO_3 (99.0%, FagaLab), Na_2CO_3 (99.0%, FagaLab), La_2O_3 (99.99%, Merck), Nb_2O_5 (99.9%), and TiO_2 (99.8%, Riedel de Haën). The mixture of green powders was milled in ethanol in an agate mortar for 3 h and then calcined at 800 ℃ for 5 h. Next, the material was milled for 12 h and calcined again under the same conditions. The formation was performed by pressing green ceramic pellets at 10 MPa and 80 MPa. Finally, the samples were sintered at two representative temperatures 1100 ℃ and 1190 ℃ for 5 h in a sealed alumina crucible. The nomenclature used for the samples is shown in Table 1.

The crystalline structure of the samples was obtained by X-ray diffraction (XRD) measurements using a Rigaku Dmax-2100 diffractometer with cobalt radiation ($\lambda K\alpha_1/\lambda K\alpha_2 = 1.78899$ Å/1.79284 Å) and 2θ in the range from 10° to 90°, working at 30 kV and 16 mA. Environmental scanning electron microscopy (ESEM) was carried out on the cross section of fragmented samples, using a Philips microscope, model ESEM XL30, operating at 15 kV and 16 mA.

In this study, the photoluminescence (PL) spectra were measured on a Jobin Yvon Horiba Fluoromax-3 spectrofluorometer, applying four excitation energies: 325, 373, 457, and 500 nm. The measurements were performed on ceramic discs of about 2 mm thickness. The determination of the band gap energy was obtained through optical absorption measurements using a UV–Vis spectrometer QE65000 Ocean Optics, in the diffuse reflectance measurement; the data was processed by the Kubelka–Munk function:

$$F(R'_\infty) = \frac{(1-R'_\infty)^2}{2R'_\infty} = \frac{\alpha}{S} \quad (1)$$

$$R'_\infty = \frac{R_\infty(\text{sample})}{R_\infty(\text{standard})} \quad (2)$$

where $R_\infty = I/I_0$ is the diffuse reflectance at one wavelength from an opaque sample with infinite thickness (> 2 μm), $0 < R_\infty < 1$; α is the absorbance in cm^{-1}; and S is the scattering factor, which is assumed to be independent of the wavelength [9,10]. The square of the absorption coefficient (α^2) as a function of photon energy ($h\nu$) was used to experimentally determine E_g. All measurements were performed at room temperature.

Table 1 Nomenclature used for the samples for each pressure and sintering temperature

Sample	Formation pressure (MPa)	Sintering temperature (℃)
KNN801100	80	1100
KNN801190	80	1190
KNN101100	10	1100
KNN101190	10	1190

3 Results and discussion

3.1 Microstructural characterization

The phase identification was carried out with XRD by the powder method. Klein *et al.* [11] have demonstrated the presence of the monoclinic phase at room temperature. Samples evidence the presence of three phases, although the monoclinic phase is the majority phase. All samples show similar diffraction patterns.

In Fig. 1(a), XRD pattern determinated by Rietveld method using Fullprof program shows the presence of two phases at room temperature: monoclinic phase ($(K_{0.5}Na_{0.5})_{0.95}La_{0.05}Nb_{0.9}Ti_{0.05}O_{2.9}$, SG = 6, $P1m1$) and hexagonal phase (La_2O_3, SG = 194, $P63/mmc$) in sample KNN801100. The lattice parameters obtained for the monoclinic phase are $a = 7.9342$ Å, $b = 7.9022$ Å, $c = 7.7676$ Å, $\alpha = \gamma = 90°$, and $\beta = 90.308°$, and for hexagonal phase, $a = b = 3.9684$ Å, $c = 6.4299$ Å, $\alpha = \beta = 90°$, and $\gamma = 120°$.

For the sample KNN801190, the phases observed at room temperature are monoclinic phase ($(K_{0.5}Na_{0.5})_{0.95}La_{0.05}Nb_{0.9}Ti_{0.05}O_{2.9}$, SG = 6, $P1m1$) and orthorhombic phase ($La_4Ti_9O_{24}$, SG = 70, $Fddd$). The lattice parameters obtained for monoclinic phase are $a = 7.9479$ Å, $b = 7.8981$ Å, $c = 7.8248$ Å, $\alpha = \gamma = 90°$, and $\beta = 90.73°$, and for orthorhombic phase, $a = 14.1458$ Å, $b = 35.5267$ Å, $c = 14.5794$ Å, and $\alpha = \beta = \gamma = 90°$.

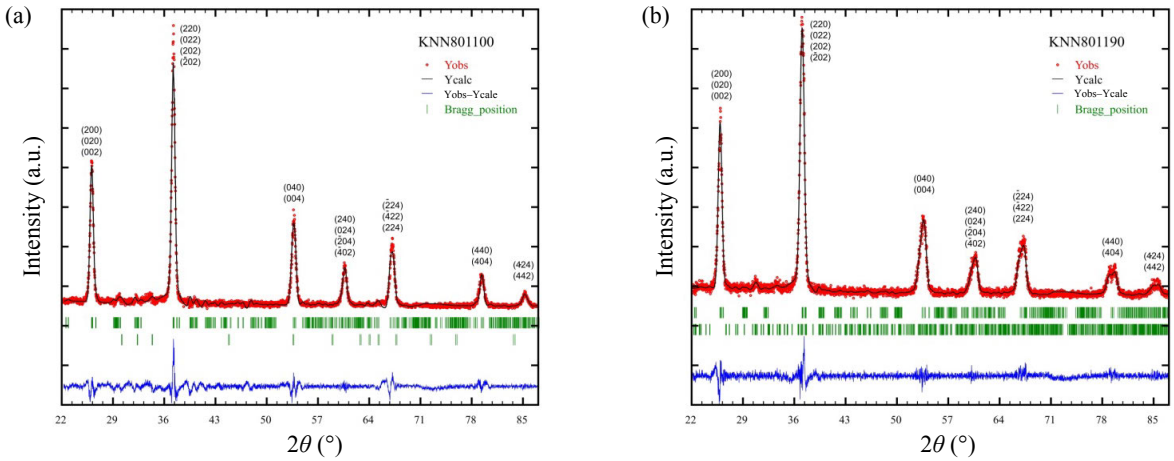

Fig. 1 XRD patterns of KNNLaTi for (a) KNN801100 and (b) KNN801190 samples, showing the results of the adjustment obtained with the Rietveld method and the difference between the experiment and adjustment.

The microstructure was analyzed by ESEM; the images obtained for all samples are shown in Fig. 2. In samples KNN801100 (Fig. 2(a)) and KNN801190 (Fig. 2(b)) obtained at higher pressure, the grains are plate-like staked of micrometer size. However, in the samples formed at lower pressure, KNN101190 (Fig. 2(c)) and KNN101100 (Fig. 2(d)) agglomerates are observed, which are constituted by grains of mainly oval shape of about 30 nm in size. All four samples are observed to be dense.

3. 2 Photoluminescence spectra and band gap energy

According to Eqs. (1) and (2), we obtained the relationship of the absorption coefficient (α) and the photon energy ($h\nu$). Figure 3 shows $(\alpha/S)^2$ versus photon energy curves; E_g is obtained graphically by the tangent to the curve at the zone where the absorption of the material decays. The samples show similar values in band gap energy, $E_g = 3.36$ eV, except for the sample KNN801190, $E_g = 3.09$ eV. Besides this difference in the value of E_g, this sample also shows a marked different value for α/S. It was expected that samples with the same composition present equal energy gaps. We assume that this difference is due to the higher sintering pressure during formation.

For the PL response, all samples were excited at 325, 373, 457, and 500 nm; two of these wavelengths (325

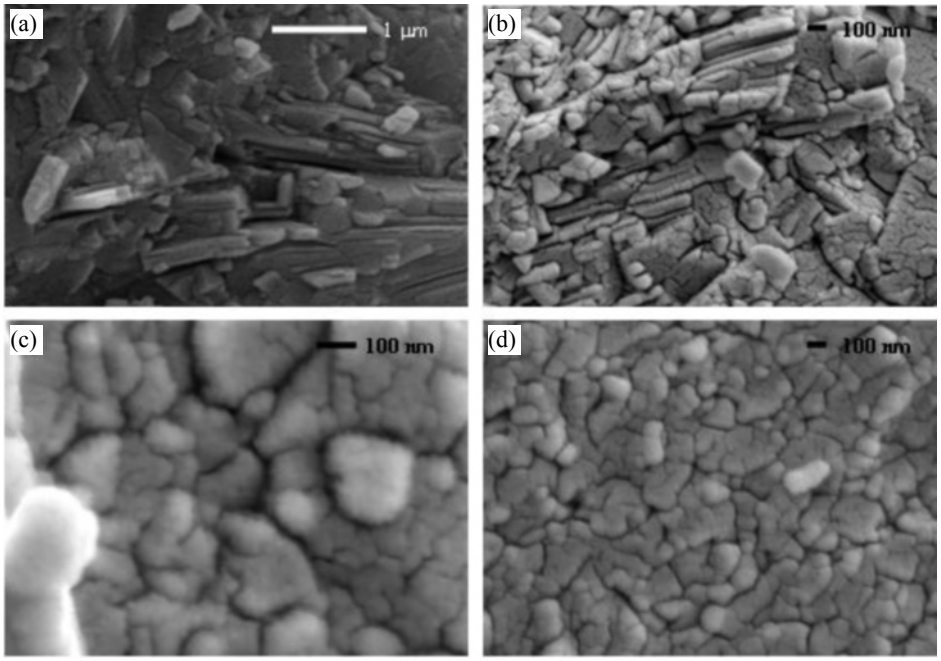

Fig. 2 ESEM images of La and Ti modified $KNaNbO_3$ ceramics sintered at different temperatures and pressures: (a) KNN801100, (b) KNN801190, (c) KNN101190, and (d) KNN101100.

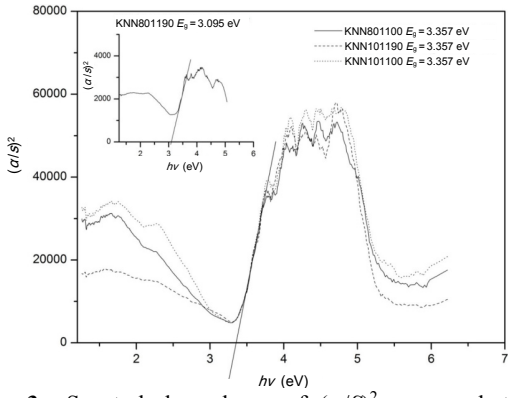

Fig. 3 Spectral dependence of $(\alpha/S)^2$ versus photon energy for all the samples.

and 373 nm) are above the band gap and the other two are within the same. For the excitation band at 325 nm (3.82 eV) (Fig. 4 left), two bands are observed: one at 3.39 eV (365 nm), which is associated with "hot excitation" emission, and the other appearing between 2.19 and 2.28 eV (566 and 544 nm), except for the KNN101190 sample, where a very intense band appears in the region of 1.98 eV (626 nm), two orders higher than all the others. When the samples are excited at 373 nm (3.32 eV) (Fig. 4 right), two zones appear as well: one around 3.00–3.08 eV (~405 nm) associated with band to band recombination, and the other with lower intensity around 1.86 eV. These results are very similar for all the samples. In PZT, these emission bands are associated with Pb^{2+} vacancies; in this case, it would be associated with Na^{+} and/or K^{+} vacancies.

Exciting all samples at 457 nm (2.71 eV) (Fig. 5 left) shows a well-defined band at 2.5 eV (496 nm), which is of similar intensity to the band–band recombination. The band at 2.5 eV is associated with materials as PZT with oxygen vacancies in the forbidden band gap, and there is another band at very low intensity at 1.81 eV

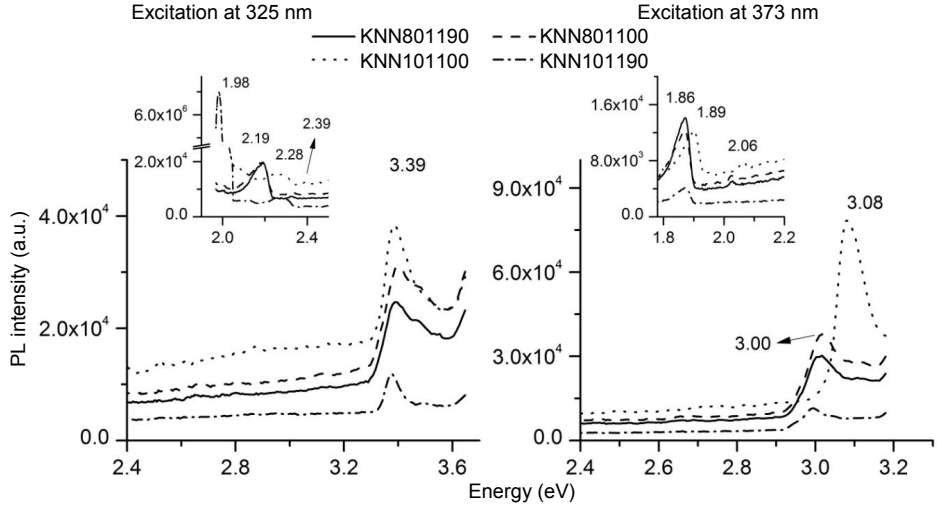

Fig. 4 PL emission spectra for all samples excited at 325 and 373 nm.

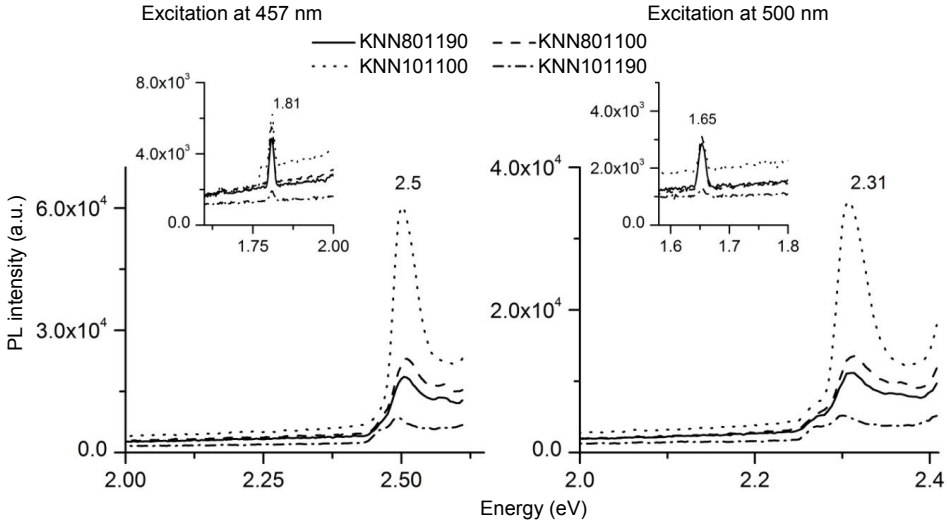

Fig. 5 PL emission spectra for all samples excited at 457 and 500 nm.

(670 nm) associated with Na^+ and/or K^+ vacancies.

The last excitation band is at 500 nm (2.47 eV) (Fig. 5 right), similar to the spectra shown in Fig. 6. The emission band at 2.31 eV (539 nm) shows high intensity and may be associated with double ionized oxygen vacancies [12].

From the permittivity measurements with temperature in the samples, AC conductivity was calculated. This allowed determining the conductivity mechanisms that are present at temperatures above the Curie temperature T_C. The results indicate that the AC conductivity is due to oxygen vacancies.

The activation energy (E_a) obtained for this process is 1.0 eV. This value corresponds to energy levels in the band gap [7,13]. The existence of these levels allows the recombination by radiative process, giving place to the emission bands that can occur in the samples (Fig. 6) in accordance with the experimental observed results (Figs. 4 and 5).

The results obtained from luminescence and UV–Vis, in conjunction with conductivity calculation, show that the existence of energy levels in the forbidden gap is associated with single and double oxygen ionized vacancies (close to the conduction band) and single and double ionized vacancies in the A site of perovskite structure (close to the valence band).

The levels of energy from single ionized oxygen vacancies are located at 0.4–0.5 eV near the conduction band, obtained from conductivity calculations. The value for double ionized oxygen vacancies is about 0.81 eV. These results agree with the theoretical results of Park [14]: the calculation results indicate that the oxygen vacancy should be easily ionized during its movement, because the defect level becomes shallow and the energy barrier for migration is significantly reduced. The large external switching electric field makes the electrons escape from the vacancy during the migration. The ionization of the oxygen vacancy during the migration provides an explanation for the charge capture process of the vacancy during the repetitive polarization switchings.

The value for single ionized vacancies in A site is 0.47–0.51 eV, and for double ionized vacancies in A site, it is 0.63 eV above the balance band. We considered the optical properties of extrinsic electrons in these two regimes separately.

Samples KNN801100 and KNN801190 have a similar behavior for all the wavelengths used, showing very low emission intensity in all observed bands compared to the PL spectra of PZT-based ceramics [2]. The sample KNN101190 also shows low intensity of emission except at 1.98 eV, which has the highest emission, two orders higher than the band–band emission. These results show an interesting possibility of application of emission wavelengths at 626, 536, 496, and 401 nm that correspond to the light orange–yellow, blue, blue–violet, and violet regions of the visible spectrum, respectively. In contrast, other authors have reported that KNN samples doped with Li and Ta have a broad emission band centered at 2.22 eV (557 nm) at 12 K, when they are excited with 325 nm [15]. Then the KNN system offers several possibilities to improve the emission characteristics through controlling the kind and concentration of dopants.

To evidence the possibility of application of the obtained emission and the magnitude of the same one,

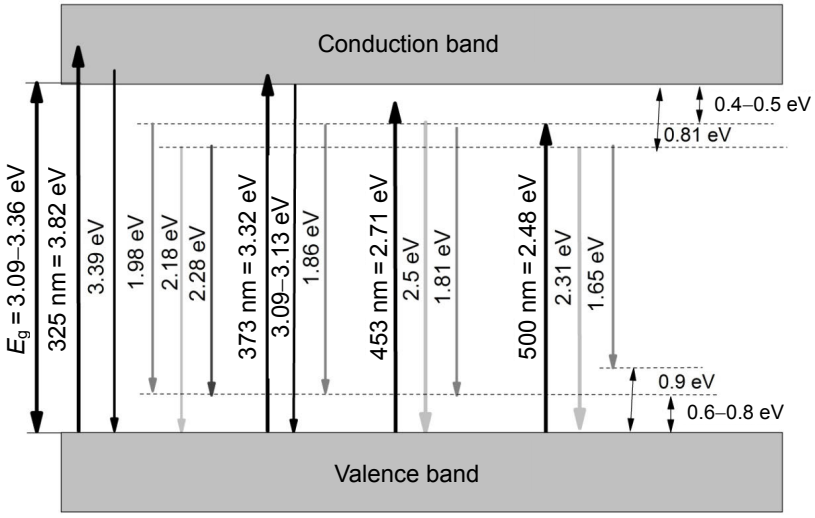

Fig. 6 Possible recombination processes in KNNLaTi ceramics. Samples were excited with different wavelengths (323, 373, 457, and 500 nm). The energy of the "gap" E_g is 3.09–3.36 eV.

it is evaluated with a Newport power meter mod. 1815-C. The power of the incident radiation and the corresponding power of emission of the sample KNN101100 for excitation wavelength at 325 and 457 nm are presented in Table 2 and Fig. 7. In Fig. 7, the blue emission is very intense in both cases.

4 Conclusions

The effect of sintering temperature and forming pressure allows obtaining samples with nanometer grain size using traditional ceramic process, providing the most economical way to get this kind of material. The samples show similar values of band gap energy, $E_g = 3.36$ eV, except for KNN801190, $E_g = 3.09$ eV. Apparently, the high temperature and pressure of the formation reduce the energy of the band gap from 3.36 to 3.09 eV. However, this decrease in band gap energy can lead to increased energy levels near the conduction and valence bands of the perovskite structure, as predicted by others.

All samples exhibit the effect of luminescence; the sample obtained at lower pressure and sintering temperature (KNN101100) has higher emissions for different excitations. The most interesting emissions of intensity appear at 1.98, 2.31, 2.5, and 3.09–3.13 eV and correspond to the emission regions orange–yellow, blue, blue–violet, and violet light spectra.

Table 2 Light power for excitation lamp and KNN101100 at different excitation wavelength

$\lambda_{excitation}$	Light power (μW)	
	Lamp	Sample
325	15.5	0.068
373	29.7	0.12
457	75.7	0.73
500	69.6	0.78

Acknowledgements

This research was supported by the project PI-ICIMAF 10/11, Cuba. Postdoctoral and Sabbatical Program for the consolidation of research groups of Conacyt. M. D. Durruthy, M. Hernández-García, and J. M Yáñez are grateful for the financial support from Conacyt-ICTP-SMF and DGAPA-UNAM for the research grant for J. Fuentes. Finally the authors acknowledge the facilities of the national laboratory for the research and development in advanced coatings, LIDTRA CONACYT 123630.

References

[1] Peng D, Sun H, Wang X, *et al*. Red emission in Pr doped $CaBi_4Ti_4O_{15}$ ferroelectric ceramics. *Mat Sci Eng B* 2011, **176**: 1513–1516.

[2] Durruthy-Rodríguez MD, Costa-Marrero J, Hernández-García M, *et al*. Photoluminescence in “hard” and “soft” ferroelectric ceramics. *Appl Phys A* 2010, **98**: 543–550.

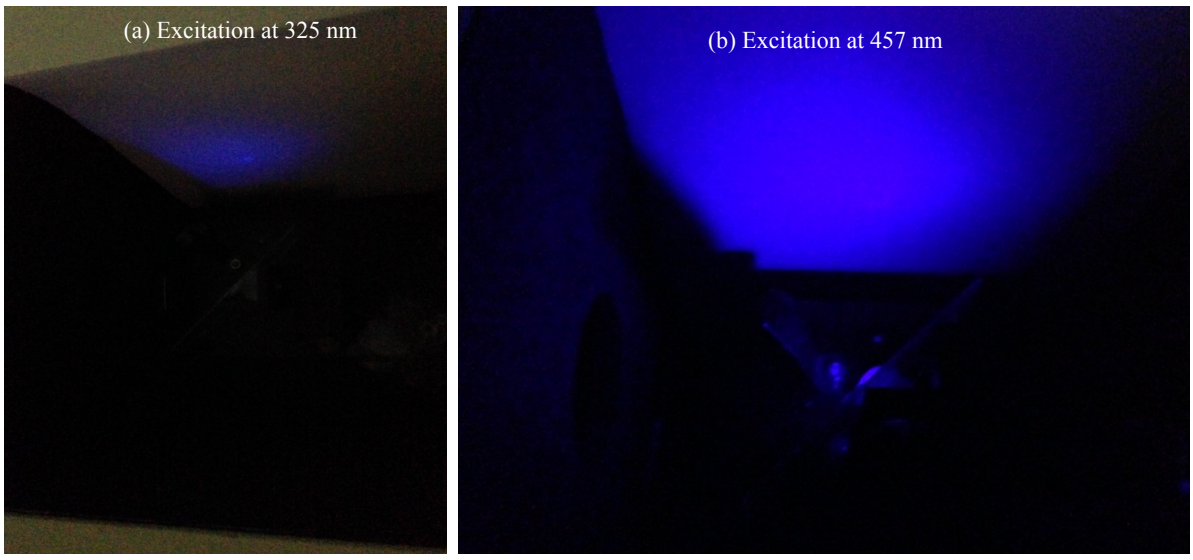

Fig. 7 Emission of KNN101100 sample for 325 and 457 nm excitation.

[3] Baedi J, Hosseini SM, Kompany A. The effect of excess titanium and crystal symmetry on electronic properties of $Pb(Zr_{1-x}Ti_x)O_3$ compounds. *Comput Mater Sci* 2008, **43**: 909–916.

[4] Baedi J, Benam MR, Majidiyan M. First-principles study of the effect of La substitution on the electronic and optical properties of $Pb(Zr_xTi_{1-x})O_3$ crystal. *Phys Scr* 2010, **81**: 035701.

[5] Stashans A, Maldonado F. A quantum mechanical study of La-doped $Pb(Zr,Ti)O_3$. *Physica B* 2007, **392**: 237–241.

[6] Anicete-Santos M, Silva MS, Orhan E, *et al*. Contribution of structural order–disorder to the room temperature photoluminescence of lead zirconate titanate powders. *J Lumin* 2007, **127**: 689–695.

[7] Fuentes J, Portelles J, Pérez A, *et al*. Structural and dielectric properties of La- and Ti-modified $K_{0.5}Na_{0.5}NbO_3$ ceramics. *Appl Phys A* 2012, **107**: 733–738.

[8] Durruthy-Rodríguez MD, Gervacio-Arciniega JJ, Portelles J, *et al*. PFM characterization of $(K_{0.5}Na_{0.5})_{0.95}La_{0.05}(Nb_{0.9}Ti_{0.05})O_{2.9}$ ceramics lead free. *Appl Phys A* 2013, **113**: 515–519.

[9] Kottim G. *Reflectance Spectroscopy*. New York: Springer Verlag, 1969.

[10] Wendlandt WW, Hecht HG. *Reflectance Spectroscopy*. New York: Wiley Interscience, 1966.

[11] Klein N, Hollenstein E, Damjanovic D, *et al*. A study of the phase diagram of $(K,Na,Li)NbO_3$ determined by dielectric and piezoelectric measurements, and Raman spectroscopy. *J Appl Phys* 2007, **102**: 014112.

[12] Kao KC. *Dielectric Phenomena in Solids*. San Diego, USA: Elsevier Academic Press, 2004.

[13] Yu PY, Cardona M. *Fundamentals of Semiconductors*: *Physics and Materials Properties*, 4th edn. New York: Springer, 2010.

[14] Park CH. Microscopic study on migration of oxygen vacancy in ferroelectric perovskite oxide. *J Korean Phys Soc* 2003, **42**: S1420–S1424.

[15] Yao Y. Studies of ferroelectrics films using micro-Raman spectroscopy and photoluminescence measurements. Ph.D. Thesis. Hong Kong: Hong Kong Polytechnic University, 2009.